Geomechanics and Engineering, *Vol. 28, No. 4 (2022) 385-396*
https://doi.org/10.12989/gae.2022.28.4.385

A computational estimation model for the subgrade reaction modulus of soil improved with DCM columns

Ali Dehghanbanadaki*[1], Ahmad Safuan A. Rashid[2], Kamarudin Ahmad[2], Nor Zurairahetty Mohd Yunus[2] and Khairun Nissa Mat Said[2]

[1]*Department of Civil Engineering, Damavand Branch, Islamic Azad University, Damavand, Iran*
[2]*Department of Geotechnics & Transportation, School of Civil Engineering, Faculty of Engineering, Universiti Teknologi Malaysia, 81310 Johor Bahru, Johor, Malaysia*

(Received July 18, 2021, Revised November 30, 2021, Accepted December 1, 2021)

Abstract. The accurate determination of the subgrade reaction modulus (K_s) of soil is an important factor for geotechnical engineers. This study estimated the K_s of soft soil improved with floating deep cement mixing (DCM) columns. A novel prediction model was developed that emphasizes the accuracy of identifying the most significant parameters of K_s. Several multi-layer perceptron (MLP) models that were trained using the Levenberg Marquardt (LM) backpropagation method were developed to estimate K_s. The models were trained using a reliable database containing the results of 36 physical modelling tests. The input parameters were the undrained shear strength of the DCM columns, undrained shear strength of soft soil, area improvement ratio and length-to-diameter ratio of the DCM columns. Grey wolf optimization (GWO) was coupled with the MLPs to improve the performance indices of the MLPs. Sensitivity tests were carried out to determine the importance of the input parameters for prediction of K_s. The results showed that both the MLP-LM and MLP-GWO methods showed high ability to predict K_s. However, it was shown that MLP-GWO (R = 0.9917, MSE = 0.28 (MN/m^2/m)) performed better than MLP-LM (R =0.9126, MSE =6.1916 (MN/m^2/m)). This proves the greater reliability of the proposed hybrid model of MLP-GWO in approximating the subgrade reaction modulus of soft soil improved with floating DCM columns. The results revealed that the undrained shear strength of the soil was the most effective factor for estimation of K_s.

Keywords: DCM columns; grey wolf optimization; soft soil; subgrade reaction modulus

1. Introduction

A promising and effective technique for increasing the bearing capacity of soil is the deep soil mixing (DSM) method using different binders (Rashid *et al*. 2017, Park *et al*. 2019, Muttuvel *et al*. 2021).

Deep cement mixing (DCM) technique involves the mechanical mixing of the soft soil primarily with cement to form a harder material in a columnar shape in order to achieve a higher bearing capacity (Bellato *et al*. 2020, Bouassida *et al*. 2020).

It features rapid solidification, low vibration and low noise, is environmentally friendly and can be applied in a limited workspace (CDIT 2002, Frikha *et al*. 2017, Kitazume *et al*. 2020). It has been used for construction of railway tracks (Kouby *et al.* 2020, Fang *et al*. 2020), foundations for embankments (Bruce *et al*. 2013), improvement of soil stability in marine applications (Shen *et al*. 2008), in earth retention systems (Waichita *et al*. 2019) and to increase the bearing capacity of shallow foundations (Topolnicki 2016). The improvement in the total bearing capacity of soft soil improved with DCM columns depends on factors such as the undrained shear strength of the basic soil and the DCM columns, the type of applied stress as well as the installation process, cement-water ratio, curing period, area improvement ratio and the dimensions of the DCM columns (Porbaha 2000, EuroSoilStab 2002, Kitazume 2020). The DCM column arrangement, which can be of the wall, block or grid type also can affect the total bearing capacity (SCDOT 2010).

Studies have shown that there is no exact cement content for the construction of DCM columns. In Malaysia, the cement content required for DCM columns in peat soil has been documented more frequently than for clay. Arulrajah *et al*. (2018) improved the shear strength of DCM columns in soft clay in Australia with the inclusion of fly ash and slag. They showed that the addition of 15% fly ash and 5% slag could increase the UCS of the DCM columns up to 30%. The positive effects of binders such as lime, gypsum and furnace slag and their combination with cement have been reported and discussed (EuroSoilStab 2002).

Several studies have performed 1g physical modelling experimental tests to determine the extent of improvement in the ultimate bearing capacity (UBC) of soft soil stabilized with DCM columns. These physical modelling tests were performed for floating (Bergado *et al*. 1999, Rashid 2011, Rashid *et al*. 2015a, Dehghanbanadaki *et al*. 2016, Lin *et al*. 2019) and end-bearing (Rashid *et al*. 2015b, Dehghanbanadaki *et al*. 2016, Bouassida *et al*. 2020) DCM columns. Centrifuge tests at 30 g (Kitazume *et al*. 2002) and 50 g (Inagaki *et al*. 2002) also have been carried out on this

*Corresponding author, Assistant Professor.
E-mail: A.Dehghanbanadaki@damavandiau.ac.ir

ISSN: 2005-307X (Print), 2092-6219 (Online)

type of improved soil. All tests reported that both floating and end-bearing DCM columns were able to increase the UBC of soft soil significantly. It has been documented that end-bearing DCM columns increase UBC more than floating columns (Rashid 2011, Dehghanbanadaki *et al*. 2016). The rate of improvement is dependent on key factors such as the area improvement ratio and geotechnical properties of the basic soil and the DCM columns.

Generally, the subgrade modulus (K_s) of the soil is defined as (Terzaghi 1995)

$$Ks = \frac{\sigma_u}{\Delta} \quad (1)$$

where K_s (kN/m^2/m) is the modulus of subgrade reaction of the soil and σ_u (kN/m^2) and Δ (m) is the stress applied to the foundation and the settlement, respectively. Eq. (1) assumes that the elastic soil compressed by σ_u can be replaced by a bed of discrete linear springs (Winkler springs 1857). In soft soil improved with DCM columns, K_s in Eq. (1) can be modified as

$$Ks = \frac{\mathrm{UBC}}{D} \quad (2)$$

Where UBC is the ultimate bearing capacity of the stabilized soil and D is the vertical displacement of the stabilized soil at the moment of failure.

Experimental determination of the K_s of soft soil improved with DCM columns is challenging. Furthermore, to date, 1g physical modelling tests have not focused on the determination of K_s. In this regard, soft computing methods such as evolutionary algorithms, fuzzy modelling and artificial neural networks (ANNs) can be effective techniques to predict K_s. Multi-layer perceptron (MLP) models are basic ANN models that are commonly used for analysis of geotechnical engineering problems (Javadi and Rezania 2009, Amiri *et al*. 2020, Liu *et al*. 2021, Dehghanbanadaki *et al*. 2021, Xiang *et al*. 2021). It should be mentioned that in practice, the exact calculation of K_s is done using the results of the plate load test in the field. In the present research, under the different loading conditions, the UBCs derived from stress-displacement chart were considered as the applied vertical stress. Therefore, the calculated K_s in this study were based on the UBC.

2. Objectives of the study

To the author's knowledge and to date, there is no computational model for estimating of the K_s of soft soil stabilized with floating DCM columns with acceptable accuracy using different databases. In addition, the K_s of soft soil is a key parameter in design programs such as SAP (Structural Analysis Program) and SAFE (Slab Analysis by the Finite Element Method). For example, in order to simulate stabilization with DCM columns of the foundations of storage tanks and embankments in soft clay, the total stiffness of the stabilized area could be obtained using the subgrade modulus in the design software. The determination of K_s in these types of projects is important and inventible. Therefore, in this study, initially the subgrade modulus of soft soil stabilized with floating DCM columns has been calculated from 36 physical modelling tests. Then, because estimation of the K_s of this type of improved soil is complex, elaborate, and expensive, the K_s of the stabilized ground was estimated using MLPs. The grey wolf optimization (GWO) algorithm was utilized to improve the performance indices of the models. Finally, several sensitivity analyses were performed to determine the influence of the input parameters on K_s.

3. Experimental datasets

The datasets for soft soil improved with floating DCM columns were developed using experimental tests on Data-1 (Dehghanbanadaki *et al*. 2016, Dehghanbanadaki 2020), Data-2 (Rashid 2011) and Data-3 (Mat Said *et al*. 2019). Information about sample preparation and physical testing can be found in the cited references.

In Data-1, highly organic fibrous peat was improved with floating DCM columns. The peat soil was collected from the Pontian area in Malaysia. The average undrained shear strength of the 10 kPa showed that in-situ peat had low shear strength and high compressibility properties. The peat soil samples were mechanically stabilized with in-situ DCM columns at area improvement ratios of 13.1%, 19.6%, and 26.2%. In the sample preparations, it was tried to achieve a homogeneous soil with undrained shear strength (C_{us}) of approximately 10 kPa after consolidation. Therefore, the rate of applied stress during consolidation began at 2 kPa and increased to 15 kPa in approximately four days. The undrained shear strength of the soil was tested using Vane shear tests (VST) and results showed that approximately the C_{us} was the same in all part of the soil.

The DCM columns then were installed in the soil using the replacement method. A rectangular footing was placed on the stabilized area and caused to fail under stress-controlled conditions at a loading rate of 1 kPa per minute. The ultimate bearing capacities of the tests were calculated from the stress-displacement curve using the double tangent method. In Data-1, well-graded sand (S) also was added to the DCM columns.

In Data-2, Rashid (2011) stabilized the kaolin clay having an undrained shear strength of 5 to 9 kPa using floating DCM columns. Area improvement ratios of 17.3, 26.2 and 34.7 were chosen. Firstly, the basic clay was consolidated under a pre-consolidated pressure of about 2.12 kPa using a pneumatic piston over the course of a day. Then the vertical stress was increased gradually over nine days in increments of 3.125, 6.25, 12.5 and 50 kPa and was finally decreased to 5 kPa to create an over consolidation ratio of 10 for the soil. Unlike in Dehghanbanadaki *et al*. (2016), the DCM columns were constructed and cured outside the soil and were inserted into predrilled holes. The stabilized area then was loaded to failure using a rectangular footing under the strain control condition of 6.20 mm/min.

In Data-3, Mat Said *et al*. (2019) used a setup similar to Data-2 at area improvement ratios of 21.7%, 32.55% and 43.4%. In Data-1, the required cement contents were calculated by Dehghanbanadaki *et al*. (2019) to be 300 kg/m^3 of the mass of wet soil. In both Data-2 and Data-3,

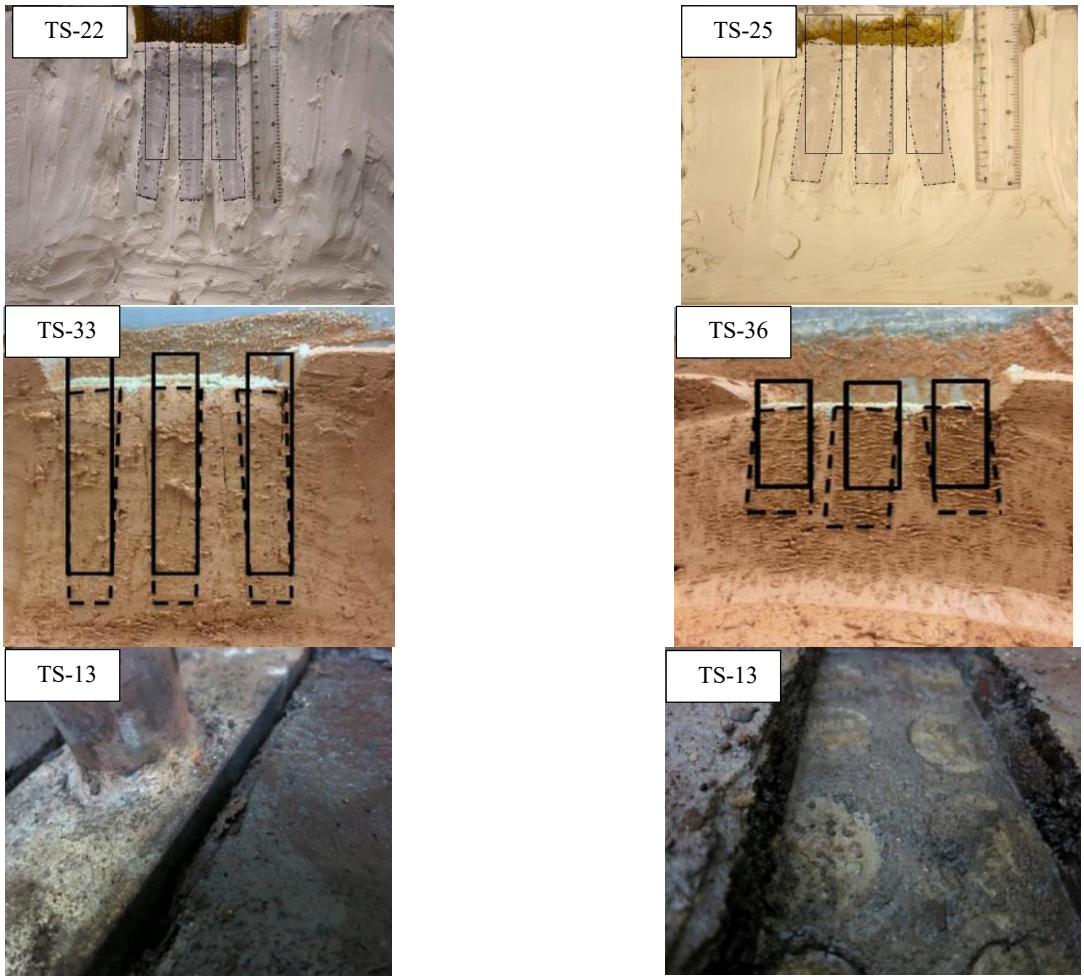

Fig. 1 Physical modelling experimental tests for computational models

Table 1 Characteristics of basic soil in physical modeling tests (Dehghanbanadaki *et al*. 2016, Rashid 2011, Mat Said *et al*. 2019)

Properties	Peat (Data-1)	Kaolin (Data-2)	Kaolin (Data-3)
OC (%)	91	--	--
Classification	Fibrous (H_3)	CL	CL
Specific gravity	1.38	2.6	2.64
LL (%)	260	63.5	57
PL (%)	160	32.2	32
PI (%)	100	31.3	25

Note: OC: organic content; LL: liquid limit; --: not applicable

the soil-cement column was prepared by mixing 85% soil and 15% cement (by weight). The geotechnical properties of the soil are shown in Table 1. Table 2 provides the details of the physical modelling tests. Fig. 2 shows a representative experimental test.

4. Computational estimation approach

In order to estimate the K_s of soft soil improved with floating DCM columns, several MLPs were created, trained and tested in MATLAB (2018). During modelling, parameters C_{us}, C_{uc}, l/d and α were chosen as inputs and the K_s was considered as the target (Table 2). Table 2 also lists the effective parameters for the loading conditions and DCM column height. The effect of DCM column height was considered in the l/d ratio. Because of the similarity principle for developing computational models, the types of loading conditions were not considered as input parameters and only parameters C_{us}, C_{uc}, l/d *and* α were used to develop the computational models. These parameters are the limitations of the proposed model and were chosen based on the recommendations of previous studies on the UBC of stabilized soils by DCMs (Porbaha 2000, CDIT 2002, EuroSoilStab 2002, Bouassida *et al*. 2020, Kitazume 2020).

The m-file was written in MATLAB using a fitting network. As a default, the Levenberg-Marquardt (LM) backpropagation algorithm (train lm function) was used to learn the rules. This algorithm minimizes the derivative of the error function with respect to the network weights and biases by changing them to a gradient-related direction. For the pre-defined parameters and based on the recommendations of the Matlab, the momentum coefficient was selected as 0.1 and the total number of epochs was as default (1000). The design of the MLP model requires the

Table 2 Data for soft soil improved with floating DCM columns

Test number	DCM columns	Loading condition	Chamber dimensions (B, L & D)	C_{us} (kPa)	C_{uc} (kPa)	DCM no	l/*d*	DCM column height (mm)	α (%)	Dataset
TS-1*	-	1kPa/min	300×200×200	9.1	-	0	-	-	-	Data-1
TS-2	Peat + C	1kPa/min	300×200×200	9.5	85.8	4	3	50	13.1	Data-1
TS-3	Peat + C + S	1kPa/min	300×200×200	9.3	65.5	4	3	50	13.1	Data-1
TS-4	Peat + C	1kPa/min	300×200×200	9.8	82.3	6	5	100	19.6	Data-1
TS-5	Peat + C + S	1kPa/min	300×200×200	9.4	69.5	6	5	100	19.6	Data-1
TS-6	Peat + C	1kPa/min	300×200×200	9.1	80.7	8	9	150	26.2	Data-1
TS-7	Peat + C + S	1kPa/min	300×200×200	9	68	8	9	150	26.2	Data-1
TS-8	Peat + C	1kPa/min	300×200×200	10.1	88.4	4	3	50	13.1	Data-1
TS-9	Peat + C + S	1kPa/min	300×200×200	9.1	65.5	4	3	50	13.1	Data-1
TS-10	Peat + C	1kPa/min	300×200×200	10.3	88.3	6	5	100	19.6	Data-1
TS-11	Peat + C + S	1kPa/min	300×200×200	10.3	64.5	6	5	100	19.6	Data-1
TS-12	Peat + C	1kPa/min	300×200×200	9.7	82.8	8	9	150	26.2	Data-1
TS-13	Peat + C + S	1kPa/min	300×200×200	9.7	66	8	9	150	26.2	Data-1
TS-14	Peat + C	1kPa/min	300×200×200	9.5	78.6	4	3	50	13.1	Data-1
TS-15	Peat + C + S	1kPa/min	300×200×200	9.5	67	4	3	50	13.1	Data-1
TS-16	Peat + C	1kPa/min	300×200×200	9.7	79.4	6	5	100	19.6	Data-1
TS-17	Peat + C + S	1kPa/min	300×200×200	9.7	62	6	5	100	19.6	Data-1
TS-18	Peat + C	1kPa/min	300×200×200	9.4	78.3	8	9	150	26.2	Data-1
TS-19	Peat + C + S	1kPa/min	300×200×200	9.4	63	8	9	150	26.2	Data-1
TS-20*	Clay + C	6.20 mm/min	400×150×430	5.7	-	0	-	-	-	Data-2
TS-21	Clay + C	6.20 mm/min	400×150×430	6.1	118.79	12	4.3	100	34.7	Data-2
TS-22	Clay + C	6.20 mm/min	400×150×430	6.2	68.98	12	4.3	100	34.7	Data-2
TS-23	Clay + C	6.20 mm/min	400×150×430	6.4	121.84	9	4.3	100	26.2	Data-2
TS-24	Clay + C	6.20 mm/min	400×150×430	6.4	87.21	9	4.3	100	26.2	Data-2
TS-25	Clay + C	6.20 mm/min	400×150×430	6.2	89.62	9	4.3	100	26.2	Data-2
TS-26	Clay + C	6.20 mm/min	400×150×430	6.4	61.88	9	4.3	100	26.2	Data-2
TS-27	Clay + C	6.20 mm/min	400×150×430	6.5	36	9	4.3	100	26.2	Data-2
TS-28	Clay + C	6.20 mm/min	400×150×430	6.3	87.66	6	4.3	100	17.3	Data-2
TS-29	Clay + C	6.25 mm/min	400×150×430	7	-	0	-	-	-	Data-3
TS-30	Clay + C	6.25 mm/min	400×150×430	7	69	6	2.1	50	21.7	Data-3
TS-31	Clay + C	6.25 mm/min	400×150×430	7	79	6	4.3	100	21.7	Data-3
TS-32	Clay + C	6.25 mm/min	400×150×430	7	54	9	2.1	50	32.5	Data-3
TS-33	Clay + C	6.25 mm/min	400×150×430	7	64	9	4.3	100	32.5	Data-3
TS-34	Clay + C	6.25 mm/min	400×150×430	7	61	12	2.1	50	43.4	Data-3
TS-35	Clay + C	6.25 mm/min	400×150×430	7	61	12	4.3	100	43.4	Data-3
TS-36	Clay + C	6.25 mm/min	400×150×430	7	69	6	2.1	50	32.5	Data-3

* = Benchmark tests; *B* = width of chamber; *L* = length of chamber; *D* = depth of chamber; C_{us} = undrained shear strength of soil; C_{uc} = undrained shear strength of column; *C* = cement; *S* = well-graded sand; *d* = diameter of DCM columns; *l* = length of DCM columns

determination of suitable architecture. When developing the MLP models, only one and two hidden layers were considered in the m-file. This decision was based on trial-and-error tests on the pre-training results. The number of neurons in each hidden layer was increased from 1 to MAX = 30 and the variations in the performance indices were monitored and evaluated during the training process. As a default of MATLAB, the data were divided into sub-groups of 70%, 15% and 15% for training, validation and testing, respectively. The nonlinear sigmoidal function was used as the transfer function in the hidden layer. For data pre-processing, all the inputs and targets were normalized to [0, 1]. This normalization process helped to speed up training and reduce the chance of getting stuck in the local optimum

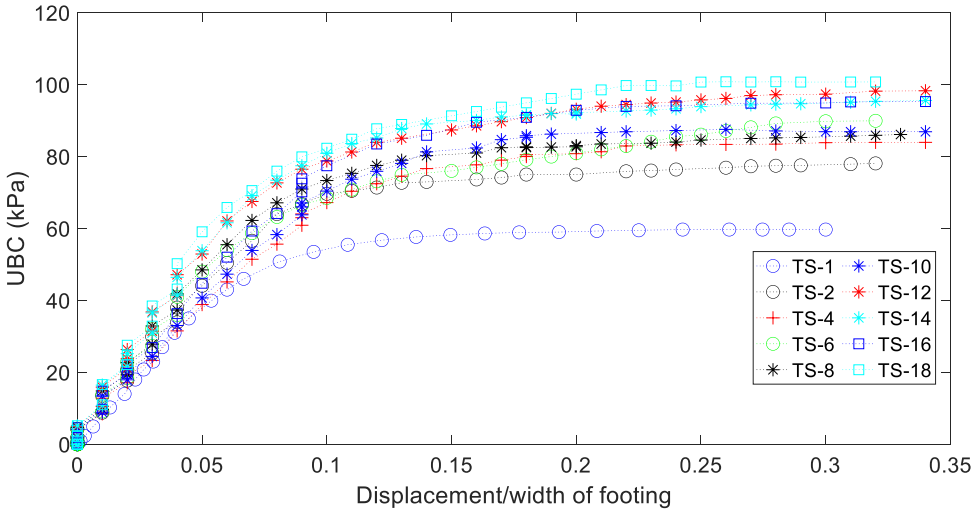

Fig. 2 Relationship between vertical stress and displacement to width of footing

(Himanshu *et al*. 2020). The performance index of MSE (mean squared error) was chosen for evaluating the accuracy of the models as follows

$$\text{MSE} = \frac{1}{n}\sum_{j=1}^{n}\left(y_j - d_j\right)^2 \quad (3)$$

where y_j is the predicted output, d_j is the desired output and n is the amount of data.

Several studies showed that GWO could enhance the convergence rate and performance indices of the MLPs (Mirjalili *et al*. 2014, Keshtkarbanaeemoghadam *et al*. 2018, Faris *et al*. 2019, Himanshu *et al*. 2020, Zhang *et al*. 2020). This swarm-based algorithm imitates the social leadership hierarchy and hunting strategy of grey wolves which was developed by Mirjalili *et al*. (2014). The source code of the GWO and the effects of the parameters can be found at http://www.alimirjalili.com/GWO.html. In addition, the details of coupling of MLPs with GWO can be found in the study of Keshtkarbanaeemoghadam *et al*. (2018).

5. Experimental results

5.1 Determination of UBC and failure patterns

Fig. 2 compares the stress–displacement responses of unimproved soil with soil reinforced with floating DCM columns in Data-1 at different area improvement ratios. In the stabilized soil with floating DCM columns, all trends showed ductile behavior. However, with an increase in the area improvement ratio and DCM column length, the differences between the trends of untreated soil and improved soil increased. These differences were the result of increased skin interaction between the DCM columns and surrounding soil. The classic double tangent method was used to determine the UBC of treated samples. In this method, the UBC was obtained at the intersection of a tangent at the beginning and one at the point of the plot at three successive and equal incremental loads, which increased the incremental settlement in the log–log plot (Dehghanbanadaki *et al*. 2016).

It was found in the failure patterns in all tests that the footing displaced the underlying soil symmetrically. For Data-1, the unimproved soil and soil improved with floating DCM columns exhibited punching shear. The stabilized area declined vertically and no heave occurred along the footing, indicating that punching shear failure occurred in these tests. In addition, the lower shear strength of the DCM columns (C_{uc}) in Data-1 compared to Data-2 and Data-3 in some tests (TS-18 and TS-19) showed that the DCM columns failed in shear mode. Similar behaviors were observed for the stabilized areas in Data-2 and Data-3. However, the DCM columns in Data-2 and Data-3 did not fail in shear mode, but simply moved about 20 mm outward relative to the DCM column top. Such movements were also observed in Data-2 and Data-3 and for longer DCM columns; however, the magnitude of the tilt or outward movement of the outer DCM columns was significantly less. The DCM columns at the center penetrated almost vertically downwards by approximately the same displacement as experienced by the footing.

5.2 Effect of DCM on UBC

Fig. 3 compares the efficiency of DCM columns installed in soft soil in terms of UBC using three databases. The UBC of soil stabilized with floating DCM columns increased significantly compared to non-stabilized soil (TS-1, TS-20, TS-29). Comparison of the databases showed that for TS-18 from Data-1 having a UBC of 78.3 kPa ranked first. The tests using Data-1 were for stabilized fibrous peat soil and was expect to have a lower UBC than stabilized clay soil. A possible explanation for the UBC value for TS-18 (α = 26.2%, C_{us} = 9.4 kPa, C_{us} = 78.3 kPa, l/d = 9) could be the higher undrained shear strength of the basic soil compared to the soil in Data-2 and Data-3. Also, because all the DCM columns were floating (not end-bearing), the role of C_{us} on the UBC was greater than for the end-bearing

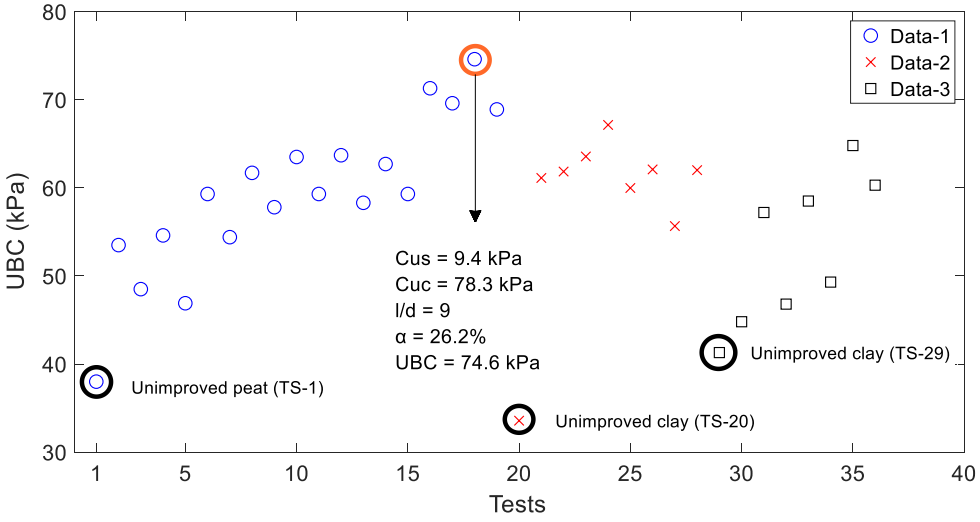

Fig. 3 Comparison of experimental UBC

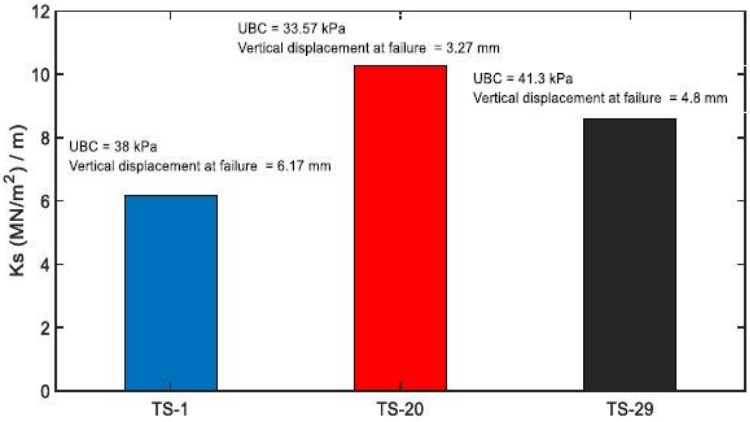

Fig. 4 Comparison of experimental K_s (non-stabilized tests)

condition. It can be seen in all datasets showing an increase in C_{us}, that an increase in C_{us}, l/d and α corresponded to an increase in UBC. For example, in Data-2, test TS-24 (α = 26.2%, C_{us} = 6.4 kPa, C_{us} = 87.21 kPa, l/d = 4.3) recorded a higher UBC of 67.14 kPa than the non-stabilized clay (TS-20) with a UBC of 33.57 kPa. The highest UBC in Data-3 was for TS-35 (α = 43.4%, C_{us} = 7 kPa, C_{us} = 61 kPa, l/d = 4.3).

5.3 Subgrade modulus of reaction analysis

Figs. 4 and 5 compare the calculated experimental K_s from tests where K_s was determined based on Eq. (2). Fig. 6 compares the K_s from the non-stabilized tests (TS-1, TS-20, TS-29). Unlike the UBCs, the K_s values for Data-2 and Data-3 (both on clay) were higher than for Data-1 on peat. The details of the UBCs and the corresponding vertical displacement are shown in Fig. 4. Fig. 5 shows and compares the K_s of all stabilized tests. Clearly, most of the tests in Data-2 and Data-3 showed higher K_s values. This confirms that, even with a lower UBC, because the corresponding vertical displacement at failure occurred at a lower level, the K_s values for clay soil were higher than for peat. In Fig. 7, the highest K_s was calculated for TS-35 at 29.72 (MN/m^2/m). This test failed at a low vertical settlement of 2.18 mm. For Data-2, the highest was for TS-27, with a K_s of 21.49 (MN/m^2/m).

A decision surface has been proposed for better estimation of K_s using the results of the experimental tests as shown in Fig. 6. In the figure, the bearing capacity (N_c) as shown in Eq. (4), and the DCM column strength ratio (K_c), as shown in Eq. (5), are the input parameters and K_s is the output parameter. As would be expected, an increase in N_c and K_c produced a corresponding increase in K_s. The equation using the linear model Poly23 is presented in Eq (14).

$$N_c = \frac{UBC}{C_{us}} \quad \text{(Bearing capacity factor)} \tag{4}$$

$$K_c = \frac{C_{uc}}{C_{us}} \quad \text{(Relative cohesion ratio of column to soft soil)} \tag{5}$$

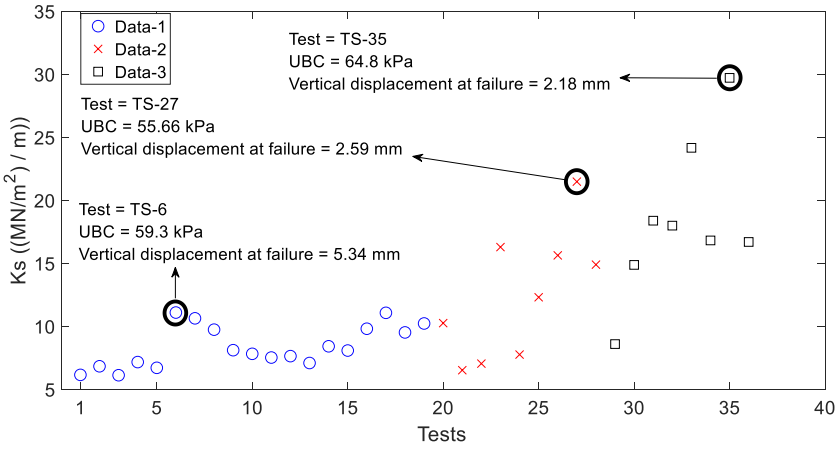

Fig. 5 Comparison of experimental K_s (improved tests)

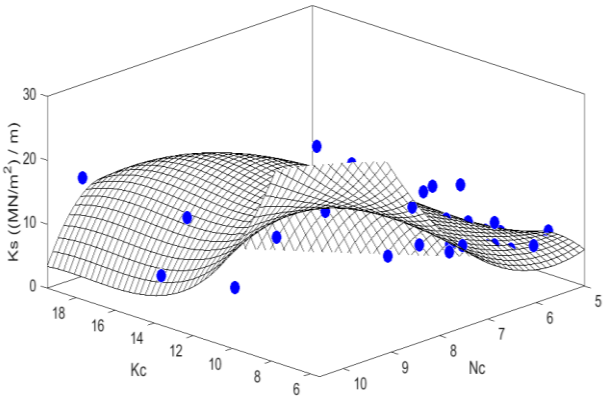

Fig. 6 Decision surface for K_s

$$K_s\,(N_c, K_c) = 154.3 - 63.25 \times N_c - 7.2 \times K_c + 6.15 \times N_c^2 + 5.63 \times N_c \times K_c - 1.23 \times K_c^2 - 0.73 \times N_c^2 \times K_c + 0.27 \times N_c \times K_c^2 - 0.03 \times K_c^3 \quad (14)$$

6. Computational estimation results

6.1 Computational models vs. experimental results

As stated, three databases were used to develop the computational models. Initially, a decision surface was developed using Poly23. Next, different MLP models were created using m-file and sensitivity analysis was performed to determine the best topology of MLPs with one and two hidden layers. Each MLP model was created, trained and tested and the performance indices were recorded. This parametric study in the decision surface in Fig. 6 and Eq. (14) showed unsatisfactory primary results (higher MSE and lower regression indices) compared to the experimental K_s and computational models. Calculations showed that the performance indices (R = 0.834, MSE = 6.68 (MN/m^2/m)) were unsatisfactory. Therefore, in the present study the focus remained on the results of the MLP and MLP-GWO models.

The basic results of computational models revealed that the models of MLP-1 (4×8×10×1), MLP-2 (4×12×1), MLP-3 (4×8×8×1), MLP-4 (4×11×1) and MLP-5 (4×13×1) performed approximately the same while MLP-4 produced slightly better results. Therefore, MLP-4 was chosen for training by GWO algorithm. Figs. 7 and 8 show the correlation coefficients of the best MLP and MLP-GWO models using MLP-4. In Fig. 8, the average correlation coefficients for all data was 0.9126 and the average MSE was 6.1916 (MN/m^2/m). By coupling the GWO with the MLP, the performance indices improved significantly.

In Fig. 8, the average of the correlation coefficients for all data increased from 0.9126 to 0.9917 and the MSE (average of all data) decreased to 0.2812 (MN/m^2/m). Notably, during the optimization process, the population size of 450, r_1 of 0.63, r_2 of 0.74 and a of 1.19 resulted the lowest MSE as the cost function. Fig. 9 shows the MSE of the best MLP-GWO model in terms of the training, validation and test data. Clearly, the lowest MSE was for the validation data at 0.1498 (MN/m^2/m). Fig. 10(a) shows the experimental K_s values and the corresponding K_s values as calculated by the best MLP model. Fig. 10(b) shows this comparison with the best MLP-GWO model. It can be concluded that, overall, with regression indices of about 99% and a very low MSE showed that the MLP-GWO model was able to estimate the K_s of the soil with floating DCM columns with high accuracy. Note that the limitations of the proposed model include the ranges of the input parameters.

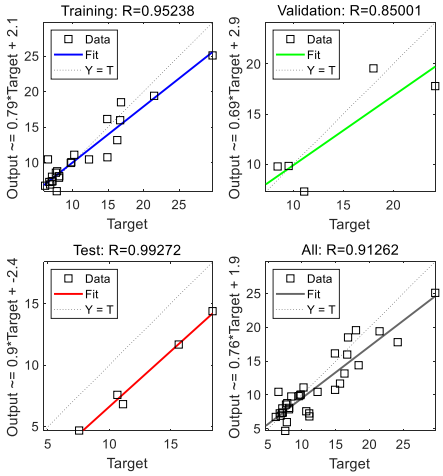

Fig. 7 Correlation coefficient of best MLP-4 (4×11×1)

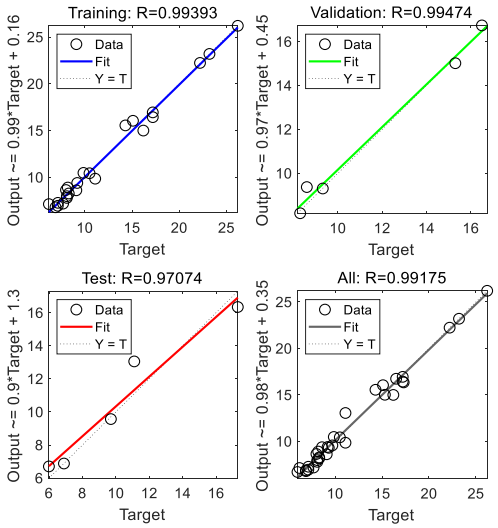

Fig. 8 Correlation coefficients of best MLP-GWO (4×11×1)

Note: Example of topology of the models: (4×8×10×1): 4 = number of input parameters; 8 = number of neurons in the first hidden layer; 10= number of neurons in the second hidden layer; 1 = number of output

7. Sensitivity analysis

For the analysis and design of soft soil improved with DCM columns, an understanding of the relative importance of each input parameter on K_s is vital. In the present study, the Garson algorithm (Garson 1991) was used for sensitivity analysis. This algorithm uses the weights and biases of all layers to rank the input parameters on the subgrade reaction modulus. The details of this algorithm are available elsewhere (Dehghanbanadaki *et al*. 2019). During the training of the models the weights and biases require updating; thus, for purposes of comparison, the best model was re-trained three times (MLP-GWO (Tr-1 to Tr-3)). Fig. 11 shows a sample of the weight and bias distributions of a MLP-GWO model called the Hinton matrix. In Fig. 11, the red color signifies a negative weight and the green color signifies a positive weight. Also, a larger box size signifies a larger number.

The weight and biases extracted from the Hinton matrix were inserted into the Garson algorithm to determine the relative importance of each input parameter on K_s. Fig. 12 shows the results of sensitivity analysis on all three computational models. As seen, all models showed approximately the same rank for the influencing factors. For example, for MLP-GWO (Tr-1), C_{us} (33%), C_{uc} (28%) and α (22%) had the greatest effects on the estimation of K_s and α (17%) had the least influence. Similar trends were observed for MLP-GWO (Tr-2) and MLP-GWO (Tr-3). The ranking of C_{us} is due to the fact that in the case of floating DCMs, since of equal vertical displacement of soil and columns at the failure moment and higher area of soils compared to the columns, the role of C_{us} was more than C_{uc}. Therefore, based on the results of sensitivity analysis of the models, it can be concluded that, in order to increase the K_s of soft soil improved with floating DCM columns, it is more efficient to increase the undrained shear of the basic soil than to do so with parameters such as the shear strength

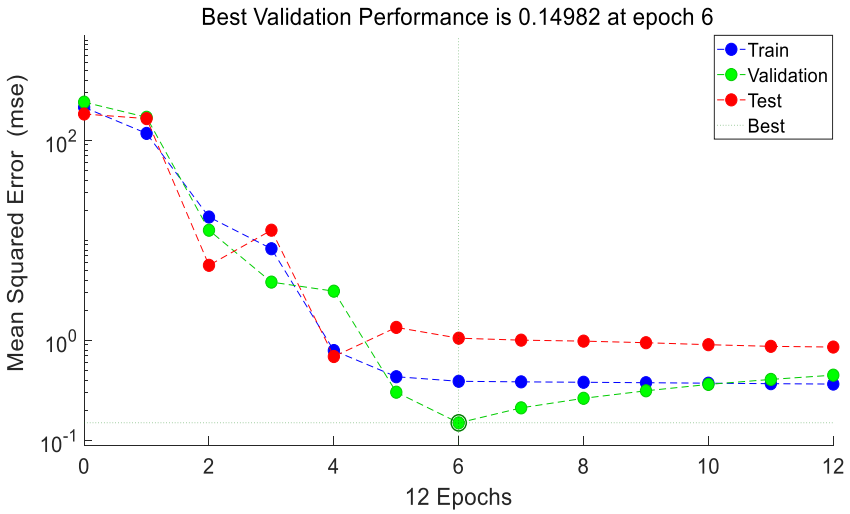

Fig. 9 MSE of best MLP-GWO model

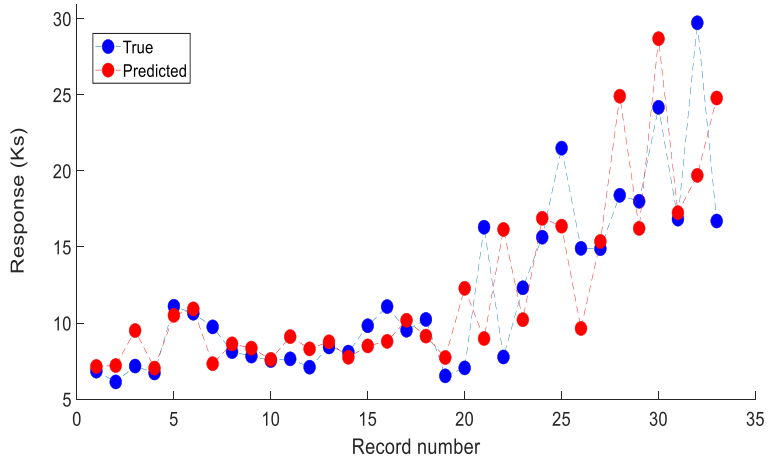

(a)

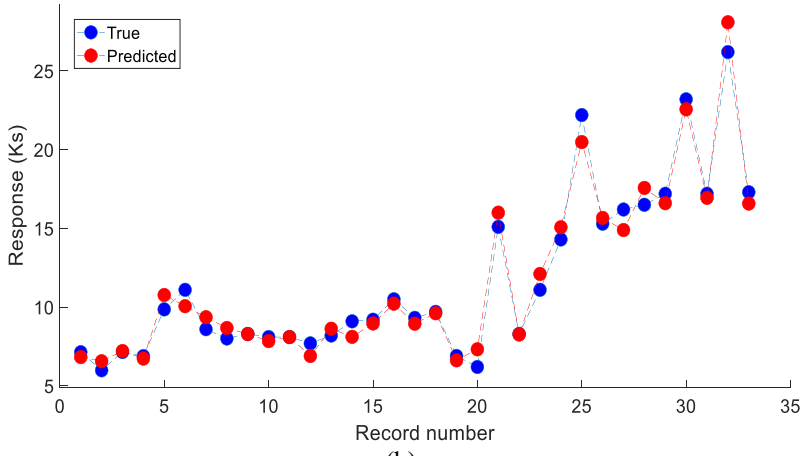

(b)

Fig. 10 Actual K_s vs. K_s estimated by proposed: (a) MLP; (b) MLP-GWO

of columns. It can be predicted that, for cases in which end-bearing DCM columns have been used, the shear strength of the columns would be the most effective parameter for K_s.

Finally, sensitivity analysis introduced C_{us} and C_{uc} as the most influential factors in the estimation of K_s of soft soils improved by floating DCM columns.

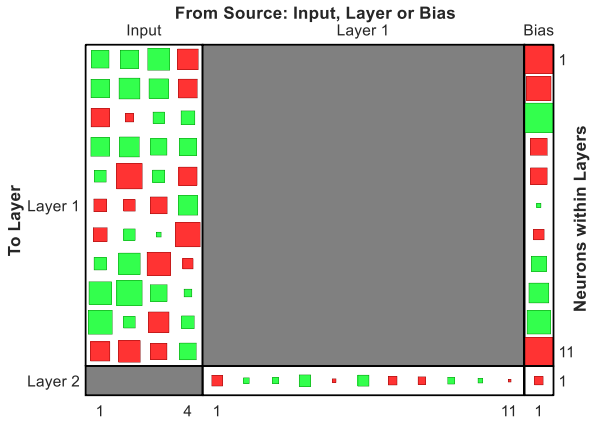

Fig. 11 Weight and bias distribution of MLP-GWO models (Hinton matrix

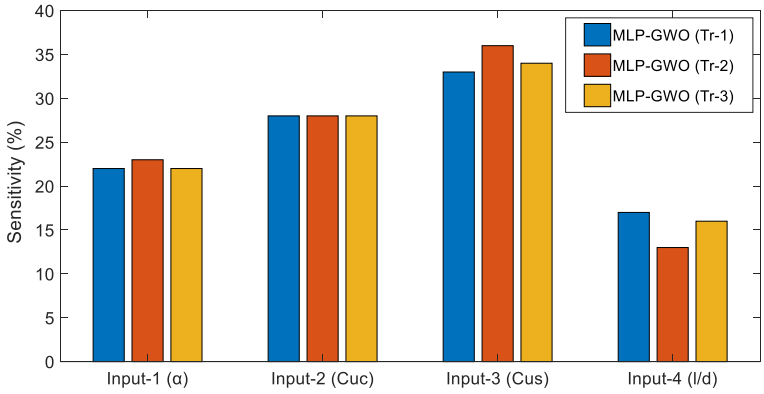

Fig. 12 Relative importance of each input variable on estimated K_s

8. Conclusions

In the present study, the subgrade reaction modulus (K_s) of soft soil improved by floating DCM columns was evaluated using the results of 36 physical modelling tests. Several multi-layer perceptron (MLPs) models then were successfully trained using the gray wolf optimization (GWO) technique to estimate K_s. When developing the models, the undrained shear strength of the soil and DCM columns, area improvement ratio and the length-to-diameter ratio of the DCM columns were used as input parameters and K_s was the target. The Garson algorithm then was utilized to determine the sensitivity of K_s to the input parameters. The results showed that in all 36 1-g physical modeling tests, the floating DCM columns increased the ultimate bearing capacity and stiffness of the composite soil, which resulted in reduced settlement and a consequent increase in K_s. Comparison of experimental results showed that, in all stabilized tests, an increase in the area improvement ratio and length-to-diameter ratio of the DCM columns produced a corresponding increase in K_s. The results of computational modeling showed that the MLP-GWO model with a topology of 4×11×1 had better performance indices than the conventional MLPs. This model had high regression indices of R =0.9917 and MSE =0.28 (MN/m^2/m). Based on the sensitivity results, it was found that for soil stabilized with floating DCM columns, the effect of the undrained shear strength of the soil was higher than for the DCM columns. It can be concluded that the proposed MLP-GWO model shows promising potential for estimation of the Ks of soft soil improved with floating DCM columns. It should be mentioned that the proposed model of this study has been developed based of the availability of data and similarity of loading and boundary conditions. Besides, the limitations of the model definitely depend on the range of input parameters and the other geotechnical properties of the soil and DCM columns.

Conflict of interest

The authors declare that there is no conflict of interest in presenting this manuscript.

Acknowledgements

This research was support by the research grants (UTMFR vote no. Q.J130000.2551.21H42) from Universiti Teknologi Malaysia in Johor Bahru, Malaysia. The second author would like to acknowledge financial support from

the Fundamental Research Grant Scheme awarded the Ministry of Education of Malaysia for the engineering and microstructural characteristics of lateritic soil treated with ordinary Portland cement under cyclic saturated (wetting) and unsaturated (drying) conditions (R.J130000.7851.5F131).

References

Amiri, S.T., Dehghanbanadaki, A., Nazir, R. and Motamedi, S. (2020), "Unit composite friction coefficient of model pile floated in kaolin clay reinforced by recycled crushed glass under uplift loading", *Transport. Geotech*., **22**, 100313. https://doi.org/10.1016/j.trgeo.2019.100313.

Arulrajah, A., Yaghoubi, M., Disfani, M.M., Horpibulsuk, S., Bo, M.W. and Leong, M. (2018), "Evaluation of fly ash-and slag-based geopolymers for the improvement of a soft marine clay by deep soil mixing", *Soil Found*., **58**(6), 1358-1370. https://doi.org/10.1016/j.sandf.2018.07.005.

Bellato, D., Marzano, I.P. and Simonini, P. (2020), "Microstructural analyses of a stabilized sand by a deep-mixing method", *J. Geotech. Geoenviron. Eng*., **146**(6), 04020032. https://doi.org/10.1061/(ASCE)GT.1943-5606.0002254.

Bergado, D.T., Ruenkrairergsa, T., Taesiri, Y. and Balasubramaniam, A.S. (1999), "Deep soil mixing used to reduce embankment settlement", *Ground Improvement*, **3**, 145-162. https://doi.org/10.1680/gi.1999.030402.

Bouassida, M., Fattah, M.Y. and Mezni, N. (2020), "Bearing capacity of foundation on soil reinforced by deep mixing columns", *Geomech. Geoeng*., 1-12. https://doi.org/10.1080/17486025.2020.1755458.

Bruce, M., Berg, R., Collin, J., Filz, G., Terashi, M. and Yang, D. (2013), "Federal highway administration design manual: Deep mixing for embankment and foundation support", (No. FHWA-HRT-13-046). Federal Highway Administation, U.S. Department of Transportation.

CDIT (Coastal Development Institute of Technology) (2002), "The Deep Mixing Method – Principle, Design and Construction, Balkelma Rotterdam, the Netherlands".

Dehghanbanadaki, A. (2020), "Intelligent modelling and design of soft soil improved with floating column-like elements as a road subgrade", *Transport. Geotech*., 100428. https://doi.org/10.1016/j.trgeo.2020.100428.

Dehghanbanadaki, A., Motamedi, S. and Ahmad, K. (2020), "Fem-based modelling of stabilized fibrous peat by end-bearing cement deep mixing columns", *Geomech. Eng*., **20**(1), 75-86. https://doi.org/10.12989/gae.2019.20.1.075.

Dehghanbanadaki, A., Ahmad, K. and Ali, N. (2016), "Experimental investigations on ultimate bearing capacity of peat stabilized by a group of soil–cement column: a comparative study", *Acta Geotechnica*, **11**(2) 295-307. https://doi.org/10.1007/s11440-014-0328-x.

Dehghanbanadaki, A., Mahdy, K., Arefnia, A., Ahmad, K. and Motamedi, S. (2019), "A study on UCS of stabilized peat with natural filler: a computational estimation approach", *KSCE J. Civil Eng*., **23**(4), 1560-1572. https://doi.org/10.1007/s12205-019-0343-4.

Dehghanbanadaki, A., Khari, M., Amiri, S.T. and Armaghani, D.J. (2021), "Estimation of ultimate bearing capacity of driven piles in c-φ soil using MLP-GWO and ANFIS-GWO models: a comparative study", *Soft Comput*., **25**(5), 4103-4119. https://doi.org/10.1007/s00500-020-05435-0.

EuroSoilStab. (2002), "Development of Design and Construction Methods to Stabilise Soft Organic Soil Design Guide Soft Soil Stabilisation; CT97-0351", Project No. BE 96-3177, Industrial & Materials.

Fang, X., Cao, C., Chen, Z., Chen, W., Ni, L., Ji, Z. and Gan, J. (2020), "Using mixed methods to design service quality evaluation indicator system of railway container multimodal transport", *Sci. Progress*, **103**(1), 0036850419890491. https://doi.org/10.1177/0036850419890491.

Faris, H., Mirjalili, S. and Aljarah, I. (2019), "Automatic selection of hidden neurons and weights in neural networks using grey wolf optimizer based on a hybrid encoding scheme", *Int. J. Machine Learn. Cy*., **10**(10), 2901-2920. https://doi.org/10.1007/s13042-018-00913-2.

Frikha, W., Zargayouna, H., Boussetta, S. and Bouassida, M. (2017), "Experimental study of Tunis soft soil improved by deep mixing column", *Geotech. Geol. Eng*., **35**(3), 931-947. https://doi.org/10.1007/s10706-016-0151-2.

Garson, G.D. (1991), "Interpreting connection neural-network weights", *Artif. Intell. Exp*., 6(7), 47-5.

Himanshu, N., Kumar, V., Burman, A., Maity, D. and Gordan, B. (2020), "Grey wolf optimization approach for searching critical failure surface in soil slopes", *Eng. with Comput*., 1-14. https://doi.org/10.1007/s00366-019-00927-6.

Inagaki, M., Abe, T., Yamamoto, M., Nozu, M., Yanagawa, Y. and Li, L. (2002), "Behavior of cement deep mixing columns under road embankment", *Proceedings of the 5th international conference on physical modelling in geotechnics: ICPMG*.

Javadi, A.A. and Rezania, M. (2009), "Applications of artificial intelligence and data mining techniques in soil modeling", *Geomech. Eng*., **1**(1), 53-74. https://doi.org/10.12989/gae.2009.1.1.053.

Keshtkarbanaeemoghadam, A., Dehghanbanadaki, A. and Kaboli, M.H. (2018), "Estimation and optimization of heating energy demand of a mountain shelter by soft computing techniques", *Sustain. Cities Soc*., **41**, 728-748. https://doi.org/10.1016/j.scs.2018.06.008.

Kitazume, M., Okano, K. and Miyajima S. (2000), "Centrifuge model tests on failure envelope of column type deep mixing method improved ground", *Soil Found*, **40**, 43-55. https://doi.org/10.3208/sandf.40.4_43.

Kitazume, M. (2020), "Keynote Lecture: Recent development of quality control and assurance of deep mixing method", In: Duc Long P., Dung N. (eds) Geotechnics for Sustainable Infrastructure Development. Lecture Notes in Civil Engineering, vol 62. Springer, Singapore. https://doi.org/10.1007/978-981-15-2184-3_69.

Le, Kouby A., Guimond-Barrett, A., Reiffsteck, P., Pantet, A., Mosser, J.F. and Calon, N. (2020), "Improvement of existing railway subgrade by deep mixing", *Eur. J. Environ. Civil Eng*., **24**(8), 1229-1244. https://doi.org/10.1080/19648189.2018.1456977.

Lin, K.Q. and Wong, I.H. (1999), "Use of deep cement mixing to reduce settlements at bridge approaches", *ASCE J. Geotech. Geoenviron. Eng*., **125**(4), 309-320. https://doi.org/10.1061/(ASCE)1090 0241(1999)125:4(309).

Liu, J., Jiang, Y., Zhang, Y. and Sakaguchi, O. (2021), "Influence of different combinations of measurement while drilling parameters by artificial neural network on estimation of tunnel support patterns", *Geomech. Eng*., **25**(6), 439-453. https://doi.org/10.12989/gae.2021.25.6.439.

MATLAB R2018b. The MathWorks: Natick, MA, USA.

Mat, Said K.N., Rashid, A.A., Osouli, A., Latifi, N., Yunus, N.Z.M. and Ganiyu, A.A. (2019), "Settlement evaluation of soft soil improved by floating soil cement column", *Int. J. Geomech*., **19**(1), 0401818. https://doi.org/10.1061/(ASCE)GM.1943-5622.0001323.

Mirjalili, S., Mirjalili, S.M. and Lewis, A. (2014), "Grey wolf optimizer", *Adv. Eng. Softw*., **69**, 46-61. https://doi.org/10.1016/j.advengsoft.2013.12.007.

Muttuvel, T., Iyathurai, S. and Ameratunga, J. (2021), "Deep soil mixing", In Soft Clay Engineering and Ground Improvement (pp. 335-358). CRC Press.

Park, J.M., Jo, Y.S. and Jang, Y.S. (2019), "Reliability assessment of geotechnical structures on soil improved by deep mixing method I: Data collection and problem setting", *KSCE J. Civil Eng*., **23**(1), 63-73. https://doi.org/10.1007/s12205-018-1135-y.

Porbaha, A. (2000), "State of the art in deep mixing technology: part IV. Design considerations", *Ground Improv.*, **3**, 111-125. https://doi.org/10.1680/grim.2000.4.3.111.

Rashid, A. (2011), "Behaviour of weak soil reinforced with soil columns formed by deep mixing method", PhD Thesis. University of Sheffield.

Rashid, A.S.A., Black, J.A. and Noor, N.M. (2015a), "Behaviour of weak soil reinforced with soil cement columns formed by the deep mixing method: Rigid and flexible footings", *Measurement: J. Int. Measurement Confederation*, **68**, 262-279. https://doi.org/10.1016/j.measurement.2015.02.039.

Rashid, A.S.A., Black, J.A., Mohamad, H. and Noor, N.M. (2015b), "Behavior of weak soil reinforced with end-bearing soil-cement columns formed by the deep mixing method", **33**(6), 473-486. https://doi.org/10.1080/1064119X.2014.954174.

Rashid, A.S.A., Bunawan, A.R. and Said, K.N.M. (2017), "The deep mixing method: bearing capacity studies", *Geotech. Geol. Eng*., **35**(4), 1271-1298. https://doi.org/10.1007/s10706-017-0196-x.

SCDOT. (2010), "South Carolina Department of Transportation", Geotechnical design manual. Chapter 19; Ground improvement.

Shen, S.L, Han, J. and Du, Y.J. (2008), "Deep mixing induced property changes in surrounding sensitive marine clays", *J. Geotech. Geoenviron. Eng*., **134**(6), 845-54. https://doi.org/10.1061/(ASCE)1090-0241(2008)134:6(845).

Terzaghi, K. (1955), "Evaluation of coefficients of subgrade reaction", *Geotechnique*, **5**(4), 297-326.

Winkler, E. (1867), "Die Lehre Von Elasticitaet Und Festigkeit 1st edition Prague: H. Dominicus".

Topolnicki, M. (2016), "General overview and advances in deep soil mixing. In: XXIV geotechnical conference of torino design,construction and controls of soil improvement systems", 25-26 February, Torino, 1-30.

Waichita, S., Jongpradist, P. and Jamsawang, P. (2019), "Characterization of deep cement mixing wall behavior using wall-to-excavation shape factor", *Tunn. Undergr. Sp. Tech*., **83**, 243-253. https://doi.org/10.1016/j.tust.2018.09.033.

Xiang, G., Yin, D., Cao, C. and Yuan, L. (2021), "Application of artificial neural network for prediction of flow ability of soft soil subjected to vibrations", *Geomech. Eng*., **25**(5), 395-403. https://doi.org/10.12989/gae.2021.25.5.395.

Yin, J.H. and Fang, Z. (2010), "Physical modeling of a footing on soft soil ground with deep cement mixed soil columns under vertical loading", *Mar. Georesour. Geotech*.; **28**(2), 173-188. https://doi.org/10.1080/10641191003780872.

Zhang, Y., Jin, Z. and Chen, Y. (2020), "Hybridizing grey wolf optimization with neural network algorithm for global numerical optimization problems", *Neural Comput. Appl*., **32**(14), 10451-10470. https://doi.org/10.1007/s00521-019-04580-4 .